Iron, Ferritin, Transferrin, and Transferrin Receptor in the Adult Rat Retina

Marina G. Yefimova,[1] Jean-Claude Jeanny,[2] Xavier Guillonneau,[2] Nicole Keller,[2] Jeanine Nguyen-Legros,[2] Claire Sergeant,[3] Florian Guillou,[4] and Yves Courtois[2]

Purpose. The retina and other tissues need iron to survive. However, the normal iron metabolism in rodent retinas had not been characterized. This study was intended to investigate iron and iron homeostasis protein (ferritin, transferrin [Tf] and transferrin receptor [Tf-R]) distribution in 20- to 55-day-old rat retinas.

Methods. Iron was revealed on retinal sections directly by proton-induced x-ray emission (PIXE) and indirectly by electron microscopy (EM). Ferritin, Tf, and Tf-R proteins were localized by immunohistochemistry. Transferrin expression was localized by in situ hybridization (ISH). Transferrin and ferritin proteins and mRNA were analyzed by Western blot analysis and reverse transcription–polymerase chain reaction (RT–PCR), respectively.

Results. Iron is widely and unevenly distributed throughout the adult rat retina. The highest concentration was observed by PIXE in the choroid and the retinal pigmented epithelial cell (RPE) layer, and in inner segments of photoreceptors (IS). Outer segments of photoreceptors (OS) also contain iron. EM studies suggested the presence of iron inclusions inside the photoreceptor discs. Choroid, RPE, and IS showed a strong immunoreactivity for ferritin. Transferrin accumulated mainly in the IS and OS areas and in RPE cells but can also be detected slightly in retinal capillaries. Western blot analysis for Tf and ferritin confirmed their presence in the adult neural retina. By RT–PCR, H- and L-chains of ferritin and Tf mRNAs were expressed in neural retina, but the main sites of Tf synthesis observed by ISH were the RPE and choroid cell layers. Tf-R immunoreactivity was detected in the ganglion cell layer, inner nuclear layer, outer plexiform layer, IS, RPE, and choroid. These results were similar for all stages studied.

Conclusions. For the first time, the present study characterized both iron and iron homeostasis proteins in rodent retinas. In the outer retina, iron and ferritin shared the same distribution patterns. In contrast, Tf, mainly synthesized by RPE cells and detected in OS and IS areas, probably helps to transport iron to photoreceptors through their Tf-R. This is a likely pathway for filling iron needs in the outer retina. (*Invest Ophthalmol Vis Sci.* 2000;41:2343–2351)

The general requirement for iron is due to its involvement in various heme and nonheme-containing enzymes, which are ubiquitously involved in cellular metabolism.[1,2] However, some peculiarities of normal retinal physiology suggest a possible particular role of iron in this tissue. First, as in the brain, the retina is surrounded by barriers that isolate it from blood supply nutrients.[3] The retinal epithelium contributes to this barrier on one side, and the neuroretinal vasculature constitutes an independent blood–retina barrier on the other side. Second, to compensate for the continuous diurnal disc shedding in the photoreceptor cells, there is extensive membrane biogenesis involving the iron-containing enzyme fatty acid desaturase.[4] Third, the iron-containing enzyme guanylate cyclase assures the synthesis of cGMP, which acts as the second messenger in the phototransduction cascade.[5] In addition, nitric oxide synthase, which probably plays a role in the rod outer segment phagocytic process,[6] also contains iron.[7] Finally, the retina is submitted to strong oxidative stress with the formation of high levels of free radicals.[8] Any overload in free iron will result in the formation of aggressive hydroxyl radicals by the Fenton reaction or peroxynitrites[7] and the subsequent death of neurons by apoptosis. Indeed, retinal dysfunctions have been observed in some pathologic states due to the lack of iron[9] or to an excess of iron.[10,11] Partial data about iron homeostasis and the synthesis or localization of the major proteins involved in this process, in the whole retina in vivo or in retinal cells in vitro, are available to date mostly for humans and chicks. Studies on the distribution of iron and iron-metabolizing proteins were performed in the chick embryo retina before and after hatching.[12–15] Trans-

From the [1]Sechenov Institute of Evolutionary Physiology and Biochemistry, Russian Academy of Sciences, St. Petersburg, Russia; [2]Développement, Vieillissement et Pathologie de la Rétine, INSERM U450, Affiliée CNRS, Association Cl. Bernard, Paris, France; [3]CNRS-URA451: Chimie Nucléaire Analytique et Bioenvironmentale, Le Haut Vigneau, BP120, 33175 Bordeaux-Gradignan, France; and [4]Institut National de la Recherche Agronomique, Physiologie de la Reproduction des Mammifères Domestiques, INRA/CNRS URA 1291, Nouzilly, France.

Supported by an INSERM fellowship (MGY) and was part of a collaborative program funded by IPSEN (Paris).

Submitted for publication July 29, 1999; revised November 30 and December 29, 1999 and February 7, 2000; accepted February 24, 2000.

Commercial relationships policy: N.

Presented in part at the annual meeting of the Association for Research in Vision and Ophthalmology, Fort Lauderdale, Florida, May, 1998.

Corresponding author: Yves Courtois, Développement, Vieillissement et Pathologie de la Rétine, INSERM U450, 29 rue Wilhem, 75016 Paris, France. ycourtoi@infobiogen.fr

ferrin (Tf) and transferrin receptor (Tf-R) have been detected in the human neural retina, retinal pigment epithelial (RPE) cells and choroid,[16–19] whereas both ferritin and a ferritin-like protein were found in cultured RPE cells of human retinas.[16] No data on ferritin distribution in the retina are available in the literature. The purpose of the present study was to investigate the distribution of iron and the main iron-metabolizing proteins ferritin, Tf, and Tf-R in fully differentiated rat retinas from the 20th to 50th postnatal (PN) day.

METHODS

Animals

Wistar, Royal College of Surgeons (RCS)-rdy, and Long–Evans rats between 20 and 55 days of age were examined. Experiments were conducted in accordance with the ARVO Statement for the Use of Animals in Ophthalmic and Vision Research.

Iron Determination

Proton-Induced X-ray Emission Studies. Eyeballs were enucleated immediately after the rats were killed, then quick frozen by immersion into isopentane, precooled at −140°C, and stored under liquid nitrogen. The frozen eyeballs were embedded in Tissue-Tek OCT, in a small cubic mold. The cubes were frozen with liquid nitrogen, then cut with a Reichert–Jung cryomicrotome at −30°C, in thin sections of 20 μm. When close to the optic nerve, thin sections parallel to the optic nerve were collected on Formvar films previously prepared on aluminum holders. Samples were freeze-dried overnight at −30°C, then stored in a desiccanter over silica gel before analysis. A detailed observation of the samples was made with an optical microscope (Zeiss, Le Pecq, France) to choose the best preserved and best located zones for analysis.

The samples were analyzed at the Bordeaux–Gradignan nuclear microprobe.[20] A 2.5 MeV proton beam of 800 to 900 pA current and approximately 5 μm in diameter was used. All specimens were irradiated for 8 to 12 hours. The scanned areas were 150 × 150 μm^2. X-rays were detected using a 80 mm^2 Si(Li) solid state detector (Link Analytical, Gif Sur Yvette, France), and backscattered protons were detected with a 20 mm^2 Si surface barrier detector placed at 135° to the beam direction. The organic mass of the analyzed samples and their thicknesses were calculated from the backscattered spectra using the RUMPIN code.[21] Fe concentrations were calculated from the x-ray intensities with the GUPIX software.[22] Special attention was paid to the elemental losses induced by proton beam irradiation of the tissue. After irradiation, the sections were stained with 1% toluidine blue and observed with an optical microscope (Aristoplan; Leica). The identification of the retinal layers in the adjacent zones allowed us to recognize them in the irradiated areas; for each layer, it was possible to get the proton-induced x-ray emission (PIXE) and RBS (Rutherford Back Scattering) spectra and then determine the iron concentration in each layer.

Electron Microscopy Studies. Anesthetized rats were perfused with phosphate-buffered saline (PBS) followed by 2.5% glutaraldehyde in 0.1 M sodium cacodylate buffer (pH 7.4). The eyes were excised and postfixed in the same solution. After 30 minutes the lens was removed, and the fixation continued for 2 more hours. The retina was cut into four quadrants and washed in 0.2 M sodium cacodylate buffer (pH 7.4) and fixed with 1% of OsO_4 in the same buffer.

In some experiments we used a modified Willingham's technique[23] to reveal iron-containing ferritin[24]: Retinal fragments were fixed as above and postfixed in the mixture of 2% K-ferrocyanide in H_2O and 2% OsO_4 in H_2O.

Post-fixation was performed in the dark for 1 hour. Samples were dehydrated in graded ethanol series of 50%, 70%, and 100% then treated in propylene oxide. After being soaked in a mixture of propylene oxide–Epon, the samples were embedded in epoxy resin. Ultra-fine sections (60–90 nm) were subjected to uranyl acetate and lead citrate except for some specimens where uranyl acetate was omitted.

Immunohistochemistry of the Ferritin, Tf, and Tf-R

Freshly enucleated eyes were fixed with 4% paraformaldehyde (PAF) in 0.1 M PBS for 2 hours and then frozen in OCT at −80°C. Frozen sections (5 μm) were cut on a freezing microtome Bright OTF/AS (D'Hondt Instruments Scientifiques; Blanc-Mesnil, France). Rabbit polyclonal antibodies against H- and L-chains of mouse recombinant ferritin were used for ferritin immunohistochemistry (dilution 1:500). We used biotinylated goat anti-rabbit secondary antibody (dilution 1:100; Byosis), then extravidin conjugated with alkaline phosphatase (dilution 1:100; Sigma). FAST-RED (Sigma) was used as its substrate. Two different primary antibodies were used for Tf immunohistochemistry: polyclonal rabbit anti-rat Tf, dilution 1:1000 (F. Guillou, INRA, France) and rabbit anti-rat Tf IgG fraction, dilution 1:500 (CAPPEL). Goat anti-rabbit immunoglobulin (IgG) secondary antibody conjugated with Pacific Blue was added for Tf immunostaining (diluted 1:100; Molecular Probes). Control nonimmune antibodies were used for each specific antibody.

A monoclonal mouse anti-rat Tf-R antibody (CD-71; Serotec, Realef, Varilhes, France) was used for Tf-R immunohistochemistry on freshly prepared unfixed OCT-embedded 5-μm-thick sections. After a brief washing in PBS, tissue sections were preincubated in 10% normal goat serum for 20 minutes to block nonspecific binding. The sections were incubated with primary antibody (dilution 1:100 in 10% goat serum/PBS) for 1 hour at room temperature. After washing in PBS the incubation with biotinylated secondary antibody (dilution 1:200) for 30 minutes at room temperature was performed. The slides were washed in PBS and incubated with extravidin–alkaline phosphatase (dilution 1:200, Sigma) for 30 minutes. After washing in PBS the FAST-RED was added as the substrate for alkaline phosphatase. Control slides were processed via the same procedure except that the monoclonal antibody against human endothelial cells clone EN7/44 (Immunotech, Luminy, France) was used (dilution 1:100).

Western Blot Analysis of Tf and Ferritin

For Western blot analysis the animals were perfused with PBS through the aorta to remove the traces of blood Tf. The neural retinas were dissected free of extraocular tissue, homogenized in 10 mM Tris–HCl buffer (pH 7.4), centrifuged 14,000*g* for 15 minutes, and 100 mg supernatant proteins were subjected to sodium dodecyl sulfate–polyacrylamide gel electrophoresis (SDS–PAGE; 12% acrylamide). Proteins were then transferred to nitrocellulose membrane (Amicon) by electroblotting. The

membrane was blocked for 2 hours at 37°C with 5% skim milk proteins in PBS and incubated with the same antibodies used in immunohistochemistry (dilution 1:1000 or 1:500 in 0.5% skim milk proteins/PBS) for 2 hours at room temperature. After washing in 1% skim milk proteins in PBS, the membrane was incubated for 1 hour at room temperature with goat antiserum to rabbit IgG conjugated to horseradish peroxidase (1:500 in 0.5% skim milk proteins in PBS). After washing with 0.5% skim milk proteins in PBS containing 0.1% Tween-20 and PBS alone, peroxidase activity was visualized using the enhanced chemiluminescence system (ECL; Amersham). Western blot analysis for ferritin followed the same procedure used for Tf analysis except that the dilution of primary antibodies for H- and L-chains was 1:500.

Determination of Tf Content by Radioimmunoassay

Transferrin was measured by radioimmunoassay.[25] Standard rat transferrin was purchased from Sigma, and the usable range of the assay was 0.2 to 200 ng/tube, with an intra-assay coefficient of variation of 8% for samples within the 20% to 70% range of specific binding. All standards and samples were assayed in triplicate.

Analysis of Tf and Ferritin Expression by Reverse Transcription–Polymerase Chain Reaction

Total RNA from the retina was isolated by the acid guanidinium thiocyanate–phenol–chloroform method.[26] One microgram of RNA was reverse-transcribed using random hexamers as primers. PCR mixes contained the supplied PCR buffer, 200 mM of each deoxynucleotide phosphate, 30 pmol of each primer, 1.25 U of *Taq* DNA polymerase (Perkin–Elmer, Courtaboeuf, France), and 1/20 of cDNA preparation in a total volume of 100 μl. To verify that equal amounts of RNA were added in each PCR reaction within an experiment and to verify a uniform amplification process, glyceraldehyde-3-phosphate dehydrogenase (GAPDH) mRNA was also amplified for each sample. PCR was carried out for 26 cycles for Tf and H- and L-chains of ferritin and 24 cycles for GAPDH. The amplified fragments were separated on a 1.5% agarose gel and transferred onto a nylon membrane (Amersham, Les Ulis, France). The number of cycles for each set of primers was adjusted to ensure exponential amplifications of cDNA at all stages studied. Specificity of the amplification process was verified by hybridization of blots with 5′^{32}P-labeled specific internal oligonucleotide probes, washed in 1× SSC, 0.1% SDS at 50°C, and exposed to x-ray films. The sequences of the oligonucleotide primers used for reverse transcription–polymerase chain reaction (RT–PCR) and those of hybridization probes are the following: Tf antisense, 5′-GGC ATC AGA CTC CAG CAT CA-3′; Tf sense, 5′-TAC CAT CAG GGC ACA GCA GC-3′; Tf hybridization probe, 5′-TGG AGT AGA CAG AAC CGC CGG C-3′; ferritin L-chain antisense, 5′-GGT TGG TCA GGT GGT TGC CC-3′; ferritin L-chain sense, 5′-CTA CCT CTC TCT GGG CTT CT-3′; ferritin L-chain hybridization probe, 5′-CCC TGG AGG CCA TGA AGG CTG -3′; ferritin H-chain antisense, 5′-CTT AGC TCT CAT CAC CGT GT-3′; ferritin H-chain sense, 5′-TGA CAA GAA TGA TCC CCA C-3′; ferritin H-chain hybridization probe, 5′-GAT GGG TGC CCC TGA AGC TGG-3′; GAPDH antisense, 5′-ATG CCC CCA TGT TTG TGA TG-3′; GAPDH sense, 5′-ATG GCA TGG ACT GTG GTC AT-3′; and GAPDH hybridization probe, 5′-GCT GAC AAT CTT GAG GGA GTT GTC ATA TTT-3′.

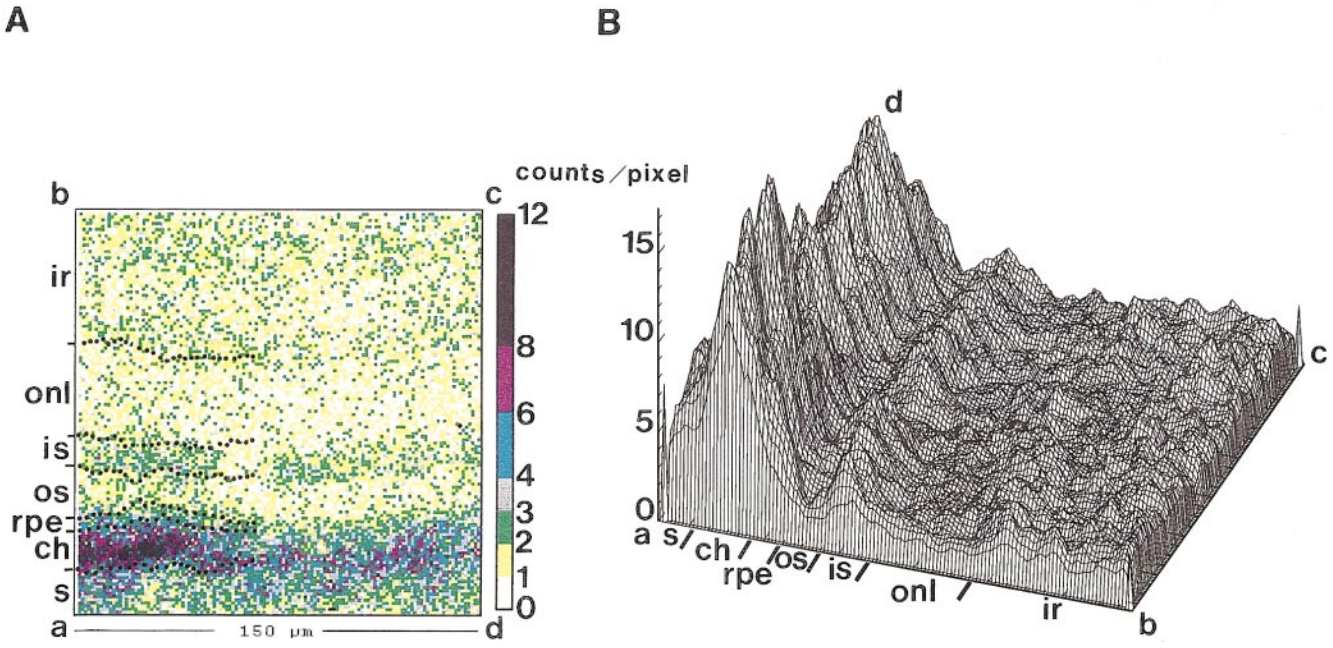

Figure 1. PIXE microanalysis of iron in PN 55-day-old rat retina. Dimensions of the scan (*square abcd*): 150 × 150 μm^2. (**A**) Bidimensional distribution map. Concentration, expressed in counts per pixel, increasing, according to the color scale, from white to black. The different retinal layers were identified after staining with toluidine blue and outlined with dotted lines. (**B**) Three-dimensional distribution map. Vertical axis represents the number of counts per pixel. From bottom to top (**A**) and from left to right (**B**) are peaks corresponding to the sclera (s), the vascularized choriocapillary layer (ch), and retina pigmented epithelium (rpe), to the inner segments (is) of the photoreceptors and to the inner retina (ir). Onl, outer nuclear layer; os, outer segments of the photoreceptors. (Figure represents the data obtained from Long–Evans strain of rats.)

Analysis of Tf Expression by In Situ Hybridization

Five-micrometer-thick unfixed OCT-embedded sections were fixed with freshly made 4% PAF in PBS (pH 7.4) for 30 minutes, rinsed in 3× PBS for 10 minutes, dehydrated through a series of ethanol treatment, then air-dried and frozen at −20°C until use. For in situ hybridization, sections were rehydrated through a graded ethanol series, rinsed in PBS, and treated in 0.02N HCl for 10 minutes. After washing in PBS, the slides were processed with 0.01% Triton X-100 for 1.5 minutes, then rinsed in PBS, and digested with proteinase K (1 μg/ml in 50 mM Tris, pH 7.4, 5 mM EDTA) for 7.5 minutes. Then slides were rinsed in PBS, containing 2 mg/ml glycine, dehydrated through graded ethanol series, and air-dried. Sections were covered overnight at 42°C with hybridization buffer (1× Denhardt, 750 mM NaCl, 25 mM Pipes, 50% formamide, 100 mM dithiothreitol, 0.2% SDS, 250 μg/ml DNA, 250 μg/ml polyA) containing 5×10^6 cpm/ml of ^{33}P-labeled antisense DNA. The control sections were hybridized with labeled sense DNA under identical conditions. The next day sections were washed twice for 10 minutes in 4× SSC, twice for 10 minutes in 2× SSC at room temperature, then rinsed in 1× SSC containing 50% formamide for 45 minutes at 45°C and in 1× SSC at room temperature before dehydration. Slides were coated with liquid nuclear emulsion K5 (ILFORD), dried, exposed at 4°C for 1 to 3 weeks, and then developed. The nucleotide sequences of the ^{33}P-labeled hybridization probes were the following: Tf-antisense, 5′-GGT GAC TCA GTG CAC ACC ATT TCA CTG GCG CGC TGT CGA TGG ACG TCC GG-3′; Tf-sense, 5′-CCG GAC GTC CAT CGA CAG CGC GCC AGT GAA ATG GTG TGC ACT GAG TCA CC-3′.

Similar results were obtained for all the rat strains considered: Wistar, RCS-rdy, and Long–Evans.

Results

Iron Distribution by PIXE Analysis and EM Studies

The PIXE technique demonstrated the distribution of total heme and nonheme iron in the adult rat retina. The RPE and choroid (178.4 μg/g dry weight) and inner segments of photoreceptors (IS; 85.3 μg/g dry weight) contain the largest amount of total iron (Fig. 1). Iron content was lower, but still significant, in the outer segments of photoreceptors (OS; 50.7 μg/g dry weight). It was much higher than in the central cornea taken as an avascular control tissue (results not shown). An indirect technique of nonheme iron detection in ferritin by a modified Willingham's assay[23] revealed very specific electron dense deposits on the disc membranes of intact photoreceptors (Fig. 2). Conversely, there were no deposits on other membranes or mitochondrial membranes. Interestingly, the same pattern was observed in phagosomes filled with partially digested disc stalks within RPE cells (Fig. 2B). Note that this technique revealed a nonspecific homogeneous staining of the intercellular space, which does not represent iron-loaded material. It is thought that this complete electron-dense filling of intercellular spaces in immersion-fixed tissue may be due to the reaction of osmium–low ferrocyanide with residual glutaraldehyde.[27,28]

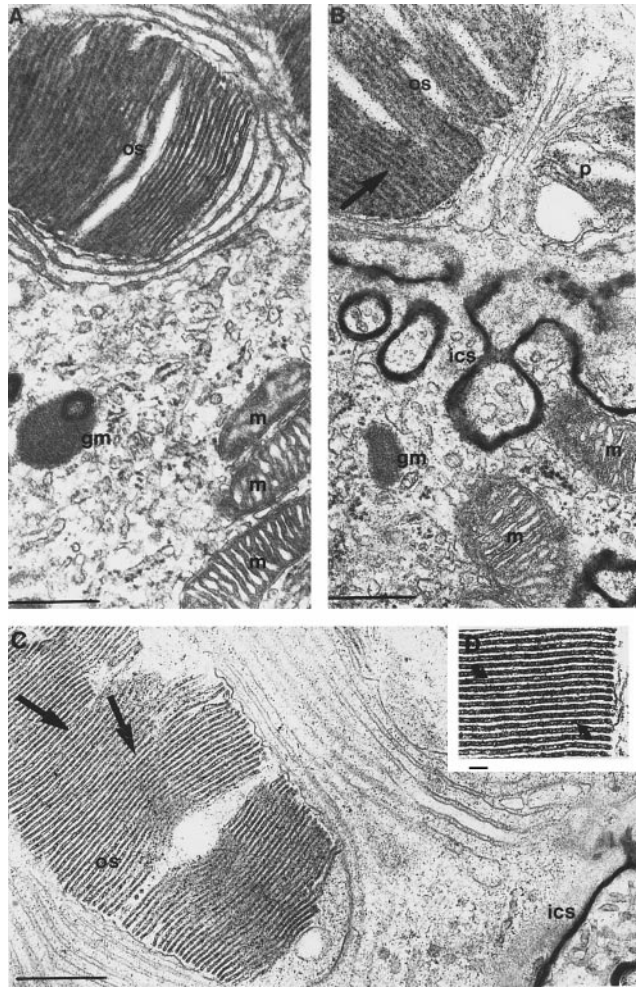

Figure 2. Electron microscopic photographs of PN 35 outer rat retina. After fixation in the absence (**A**) or presence (**B**) of K-ferrocyanide, the sections were processed as described and stained with uranyl acetate and lead citrate. Note the presence of intact outer segments (os) in apposition to RPE cells, which contain granules of melanin (gm) and mitochondria (m). In (**B**) a granular material could be observed in intact OS (*arrow*) surrounded by the plasma membrane of RPE cells and on partially digested OSs within the phagosome (p). No such granulations were observed in mitochondria. Note that some intercellular spaces (ics) exist between RPE cells and photoreceptors (**B**), which are uniformly stained. (**C**) Section of intact photoreceptor treated as in (**B**) but without uranyl acetate treatment. Note the electron dense granular material accumulated inside or associated with the disc membrane (*black arrows*). (**D**) Higher magnification than OS in (**C**). In (**B**) and (**C**) the black ics is due to the reaction of osmium-low ferrocyanide with residual glutaraldehyde and does not represent iron-loaded material. Note that in both (**C**) and (**D**) the membrane contrast was reduced due to the absence of uranyl acetate treatment. Scale bars, (**A**, **B**, **C**) 0.5 μm; (**D**) 0.1 μm. (Figure represents the data obtained from RCS-rdy strain of rats.)

Ferritin Immunolocalization, Protein Analysis, and mRNA Expression

Studies on ferritin distribution revealed the presence of its H- and L-chains throughout the adult rat retina. Both anti–H- and anti–L-immunoreactivity was detected in all retinal layers including the ganglion cell layer (GCL), inner nuclear layer (INL), IS and OS of photoreceptors, and in the choroid and around

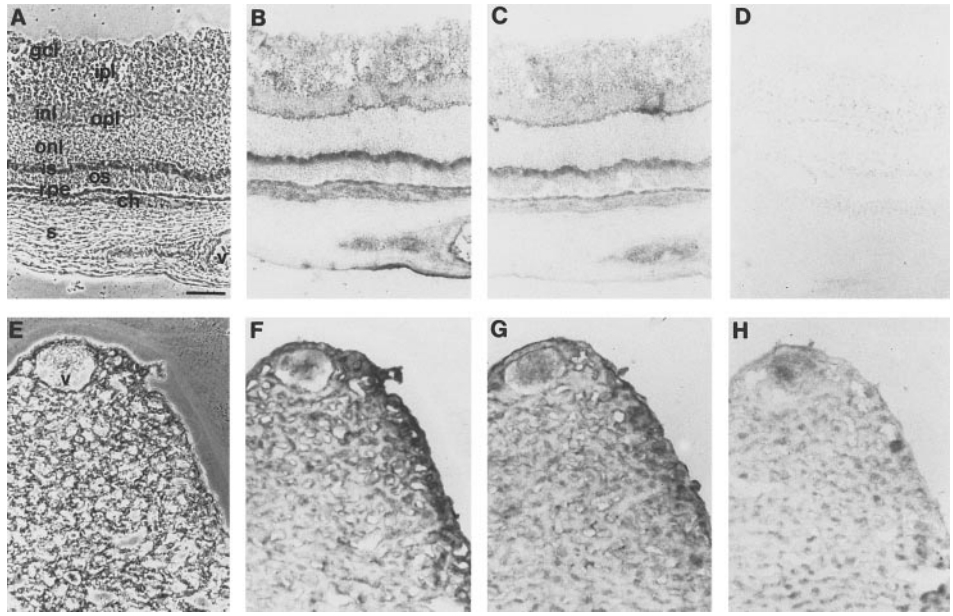

FIGURE 3. Immunolocalization of ferritin on frozen sections of PN 35 rat retina (**A** through **D**) or liver (**E** through **H**). Frozen sections were incubated with two different polyclonal antibodies against L- (**A**, **B**, **E**, **F**) or H- (**C**, **G**) ferritin subunits. Non-immune serum was used as a control (**D**, **H**). Note that the staining in (**H**) corresponds to the natural color of the blood cells. (**A, E**) phase contrast; (**B** through **D, F** through **H**) bright field. ch, choroid; gcl, ganglion cell layer; inl, inner nuclear layer; ipl, inner plexiform layer; is, inner segments of photoreceptors; onl, outer nuclear layer; opl, outer plexiform layer; os, outer segments of photoreceptors; rpe, retinal pigmented epithelium; s, sclera; v, scleral vessel. Scale bar, 70 μm. (Figure represents the data obtained from RCS-rdy strain of rats.)

the choroidal vessels (Fig. 3). The strongest immunoreactivity for H- and L-chains of ferritin was localized in the IS of photoreceptors and RPE cells. In liver sections, anti-ferritin antibodies stained the parenchyma and endothelial cells, confirming the specificity of antibodies used.

The Western blot analysis showed the presence of H- and L-chains of ferritin in perfused PN 20 and PN 40 rat retinas (Fig. 4). Because of the similarity in molecular weight of L- and H-chains of ferritin (19 and 21 kDa, respectively) and their polymerization properties, ferritin from perfused rat retinal extracts co-migrated with rat liver ferritin on 12% SDS–PAGE and Western blot analysis as a band with an apparent high molecular weight near the top of the gel. No difference was found in the expression of these proteins at the two developmental stages studied (PN 20 and PN 40). We studied the expression of H- and L-chain ferritin mRNAs by RT–PCR at PN days 20 to 50 and found no difference in expression at any stage studied (Fig. 5).

Tf Immunolocalization, Protein Analysis, and mRNA Expression

The strongest Tf immunoreactivity was detected in both the OS and IS of adult rat photoreceptors (Fig. 6). A significant Tf immunoreactivity was also seen in the thin layer of RPE cells. However, this was difficult to quantify definitively because of the small thickness of the RPE layer tightly adjacent to the strongly Tf immunoreactive vascularized choroid in nonperfused rats. Tf immunoreactivity was also found in retinal capillaries, vascularized choroid, and sclera. A very weak homogeneous background corresponding to anti-Tf immunostaining was also observed in the neural retina due to the presence of blood vessels.

Western blot analysis for Tf of the neural retina showed a band that migrates with an apparent molecular weight of 80 kDa. The content of Tf was similar in the retinas of rats at PN 20 and 40 (Fig. 7). A quantitative determination of the amount of Tf in the same extracts was determined by radioimmunoassay. Twenty-day-old and 40-day-old perfused neural retina extracts contain approximately 1.2 to 1.4 μg Tf/mg of soluble protein extract. Thus, it was of interest to look for the expres-

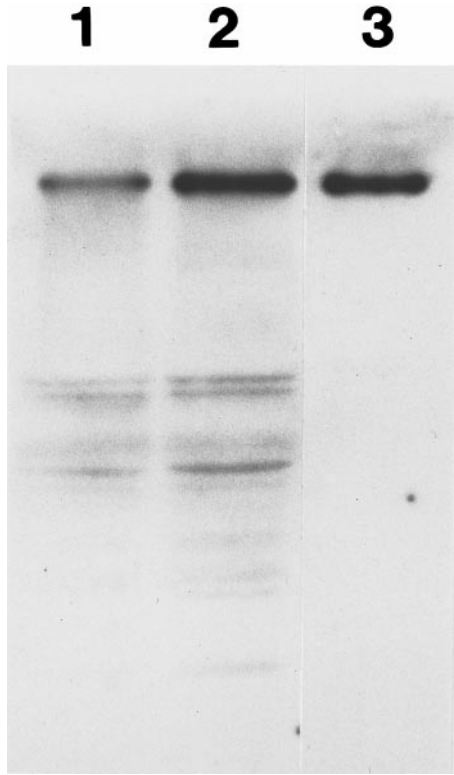

FIGURE 4. Analysis of ferritin content in rat retinal extracts by Western blot analysis. Whole extracts of perfused rat neural retina at PN 20 and 40 were subjected to SDS–PAGE, and ferritin L-subunit revealed, with the same antibody as above. Most of the ferritin remains near the top of the gel and migrates as a single band. *Lane 1:* PN 20; *lane 2:* PN 40; *lane 3:* ferritin standard. The same results were obtained for the ferritin H-subunit. (Figure represents the data obtained from Wistar strain of rats.)

FIGURE 5. Expression of ferritin mRNA by RT–PCR analysis from rat neural retina. Both H- and L-chain expression of ferritin could be observed at all stages studied of PN 20 to 50 (*top*). The amount of H- and L-ferritin subunit transcripts was compared with GAPDH transcripts expressed in the same samples (*bottom*). The experiments were performed on 3 identical mRNA preparations. (Figure represents the data obtained from RCS-rdy strain of rats.)

sion of Tf in the adult rat retina. We used the RT–PCR technique with mRNA prepared from the neural retina at different postnatal stages. As can be seen in Figure 8, the neural retina expressed Tf mRNA at all stages studied. This experiment was not performed on a freshly isolated RPE cell layer because of the difficulty to obtain it devoid of choroidal contamination. Thus, these experiments demonstrate clearly that Tf can be

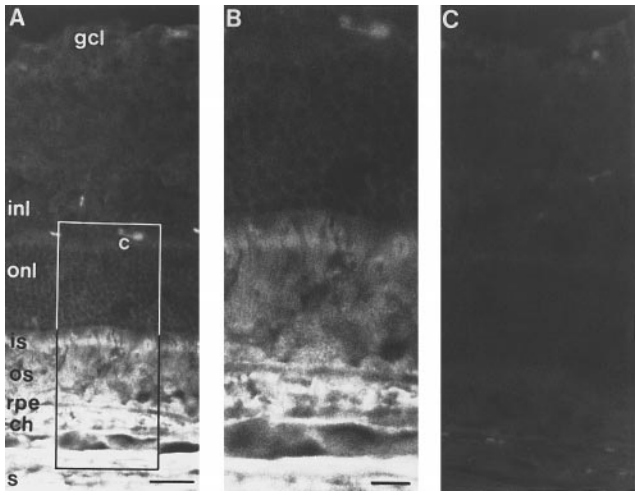

FIGURE 6. Immunolocalization of Tf on frozen sections of PN 35 rat retina. Frozen sections from PN 35 rat retina were incubated with a polyclonal Tf antibody (**A**, **B**) or with non-immune serum (**C**). (**B**) is a higher magnification than (**A**). c, capillaries; ch, choroid; gcl, ganglion cell layer; inl, inner nuclear layer; is, inner segments of photoreceptors; onl, outer nuclear layer; os, outer segments of photoreceptors; rpe, retinal pigmented epithelium; s, sclera. Scale bars, (**A**, **C**) 30 μm; (**B**) 15 μm. (Figure represents the data obtained from RCS-rdy strain of rats.)

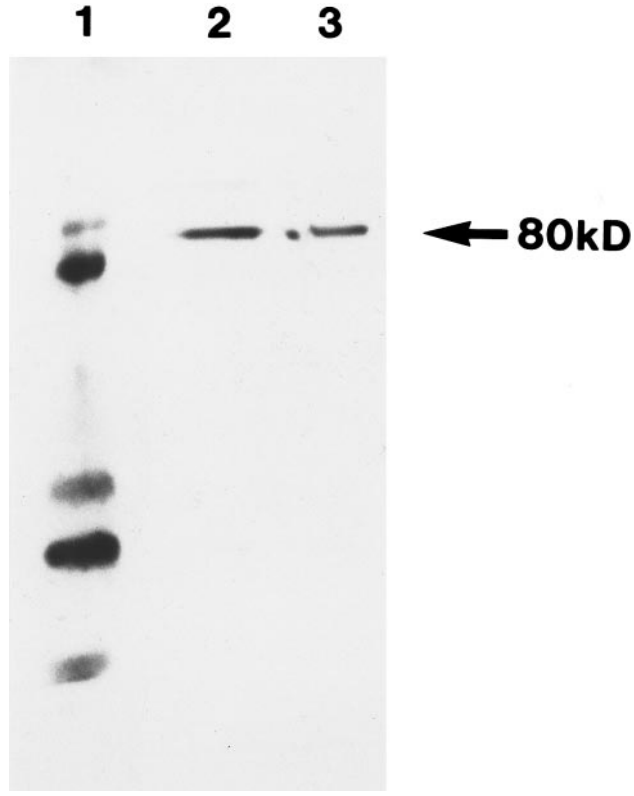

FIGURE 7. Analysis of Tf content in rat retinal extracts by Western blot analysis. Whole extracts of perfused rat retina at PN 20 and 40 were subjected to SDS–PAGE, and Tf was detected with the same antibody as above. Most of the Tf migrates as a single band with an apparent molecular weight of 80 kDa. *Lane 1:* molecular weight markers; *lane 2:* PN 20; *lane 3:* PN 40. (Figure represents the data obtained from Wistar strain of rats.)

expressed by the neural retina but leave open the identification of the cells responsible for the high amount of Tf observed by immunocytochemistry and Western blot analysis. Therefore, it was of interest to analyze by in situ hybridization the site of

FIGURE 8. Expression of Tf mRNA by RT–PCR analysis of neural retina. Tf expression could be observed at all stages studied, from PN 20 to 55 (*top*). The amount of Tf transcripts was compared with GAPDH transcripts expressed in the same samples (*bottom*). The experiments were performed on 3 identical mRNA preparations. (Figure represents the data obtained from RCS-rdy strain of rats.)

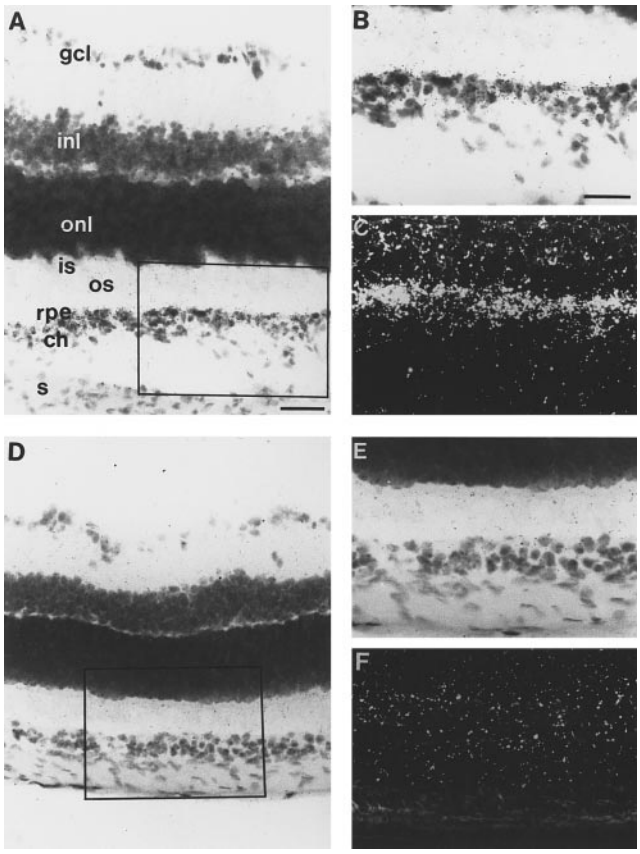

FIGURE 9. Localization of Tf expression in the PN 35 rat retina by ISH. The sections were hybridized with the antisense (**A** through **C**) or the sense (**D** through **F**) probes and visualized by autoradiography. Note that the silver grains are localized very densely on the RPE cells. (**A**, **B**, **D**, **E**) Bright field after staining with hematoxylin and eosin; (**B**, **C**, **E**, **F**) higher magnification of areas from (**A**) and (**D**), respectively; (**C**, **F**) dark field corresponding to (**B**) and (**F**), respectively. Scale bars, (**A**, **D**) 45 μm; (**B**, **C**, **E**, **F**) 30 μm. ch, choroid; gcl, ganglion cell layer; inl, inner nuclear layer; is, inner segments of photoreceptors; onl, outer nuclear layer; os, outer segments of photoreceptors; rpe, retinal pigmented epithelium; s, sclera. (Figure represents the data obtained from RCS-rdy strain of rats.)

mRNA expression on retina sections. These experiments were performed in the adult retina at the ages of PN 25, 35, and 55. As can be seen in Figure 9, the main localization for Tf mRNA expression was the RPE cell layer and, to a lesser degree, the choroid. Because very few vessels were observed in these sections of the neural retina, it was not possible to assess whether vascular cells also contribute to the production of Tf.

Immunolocalization of Tf-R in the Adult Retina

Because Tf was found mainly in the OS of the photoreceptor layer and seem to be produced mainly by RPE cells, it was of interest to determine the presence of Tf-R in the retina. These experiments were performed using a monoclonal antibody against rat Tf-R. According to the data obtained, Tf-R is widely distributed in the adult rat retina (Fig. 10). Prominent Tf-R immunoreactivity was detected in the GCL, INL, outer plexiform layer (OPL), IS of photoreceptors, RPE, and choroid and its vessels. A relatively weak anti–Tf-R immunostaining was also seen in outer nuclear layer (ONL). In liver sections, used as a positive control, the antibodies label the vessel walls and the liver parenchyma.

DISCUSSION

This work reveals the distribution of iron and its homeostasis proteins (ferritin, Tf, and Tf-R) in the adult rat retina. PIXE analysis was used to determine the principal sites of total heme- and nonheme iron localization because of its resolution compared with classic histochemical techniques. According to the data obtained in nonperfused rat eyes, the highest content of total iron was present in the choroid and RPE layers. A significant amount of iron is also detected in the IS of photoreceptor cells, INL, and GCL. Other retinal structures, including the OS of photoreceptors cells, showed some presence of iron but with lower concentrations than in the IS. The techniques used for iron determination did not allow us to reveal the valence of the iron detected (Fe^{2+} or Fe^{3+}), which could be distributed differently at the subcellular level. The distribution of the main cellular iron-storage protein ferritin (which stocks nonheme iron) follows the same pattern as iron. The strongest anti-ferritin immunoreactivity was clearly seen in the choroid, RPE cells, IS of photoreceptors, and INL and GCL. It is interesting to note that the OS of the photoreceptors shows significant anti-ferritin immunoreactivity for both H- and L-ferritin subunits. The RT–PCR studies and Western blot analysis revealed the presence of both mRNA and protein for H- and L-ferritin chains in the neural retina at all stages studied. Thus, the data obtained allow us to conclude for the first time that the iron and iron-storage protein ferritin are widely and unevenly distributed throughout the adult rat retina. Both iron and ferritin levels seem to be correlated, but the presence of iron-loaded ferritin has not been reported so far.

The retina, like other tissues, obtains iron from the circulation wherein iron is transported by the main iron-transport protein Tf. The presence of Tf-R on the surface of a variety of cells assures the binding of Tf and iron delivery into the cell via endocytosis or transcytosis.[16] Indeed, the anti–Tf-R immunoreactivity in the different retinal layers suggests the Tf-R–dependent pathway of iron uptake in both the inner and outer rat retina. It should be noted that a Tf-R–dependent mechanism of iron uptake has already been reported for human photoreceptors.[19] Our studies on Tf immunolocalization revealed weak anti-Tf immunoreactivity throughout the adult rat retina. The three main anti-Tf-immunoreactive structures of the retina were the RPE and IS and OS areas of photoreceptor cells. In situ hybridization (ISH) studies indicate that the RPE cell layer is the main site of Tf synthesis. This finding is supported by our unpublished results, which show Tf synthesis by primary cultures of rat RPE cells. It is not clear whether the strong anti-Tf immunoreactivity in the IS and OS of photoreceptors is due to its localization inside or outside photoreceptor cells. The presence of Tf-R immunoreactivity on IS of photoreceptors supports the external origin of Tf (from RPE cells); at the same time our RT–PCR and Western blot analysis data suggest the possible internal origin of Tf.

Because Tf represents one of the major soluble proteins of the intraocular fluid and is thought to be derived from intraocular sources,[29] the Tf, found in/on the photoreceptors and in/on the other cells of the neural retina, could also come from the vitreous humor via the Tf-R–dependent mechanism.[30] But

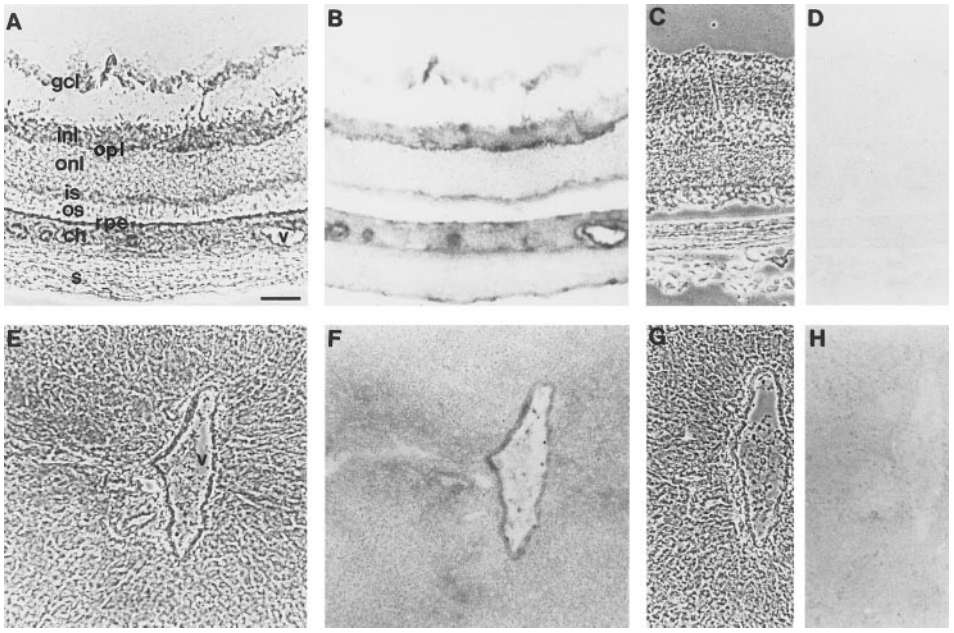

FIGURE 10. Immunolocalization of Tf-R on frozen sections of PN 35 rat retina (**A** through **D**) or liver (**E** through **H**). Frozen sections were incubated with a monoclonal Tf-R antibody (**A**, **B**, **E**, **F**) or as a control with a monoclonal antibody against human endothelial cells at the same dilution (**C**, **D**, **G**, **H**). (**A**, **C**, **E**, **G**) Phase contrast; (**B**, **D**, **F**, **H**) bright field. Scale bar, 70 μm. ch, choroid; gcl, ganglion cell layer; inl, inner nuclear layer; is, inner segments of photoreceptors; onl, outer nuclear layer; opl, outer plexiform layer; os, outer segments of photoreceptors; rpe, retinal pigmented epithelium; s, sclera; v, vessel. Note that greatest anti–Tf-R immunoreactivity was present in the INL, RPE, and choroid. (Figure represents the data obtained from RCS-rdy strain of rats.)

it is unlikely that the requirement for Tf in the outer retina, as satisfied by diffusion across the inner retina from the vitreous in nonpathologic situations, is due to the presence of ocular retinal barriers. Further electron microscopy (EM) studies are in progress to clarify these questions. However, it seems obvious that, as in the brain[2,31,32] where mechanisms of Tf synthesis and Tf absorption seem to occur, these two mechanisms of compensating retinal needs of Tf (i.e., Tf synthesis by the retina and by absorption from the vitreous) are possible. It is well known that Tf can act not only as an iron-transport protein but also as growth, neurotrophic, and differentiation-promoting factors.[14,15,33] Some of these neuromodulator properties have also been attributed to the Tf in retinal tissues.[34]

It is widely accepted for the outer mammalian retina that iron originates from RPE cells.[16] The question is, what is the iron carrier from RPE to the photoreceptor cells? For the human retina, low-molecular-weight proteins were proposed to be iron carriers.[16] Our ISH data strongly indicate that the main site of Tf synthesis in the adult rat retina is the RPE cells. Thus, it seems likely that Tf, synthesized in RPE cells, could act as an iron transporter, which crosses the interphotoreceptor matrix and then delivers iron to photoreceptors via a Tf–Tf-R–dependent mechanism.

Our data on the main site of Tf synthesis in the rodent retina differ significantly from those reported in humans.[19] However, the Tf-R distribution in the IS of photoreceptors, in RPE cells in culture,[16,19] and in the neural retina shows a similar pattern. It should be noted that human RPE cells in culture[16] and rat RPE cells were immunopositive for the iron-storage protein ferritin. No data are available on iron distribution in the human normal retina except those concerning the particular cases of iron accumulation in drusen area in patients with macular degeneration.[35]

As for the posthatching chick retina, Tf followed a pattern of distribution similar to that in the rodent retina. At the same time, anti–Tf-R immunoreactivity was predominantly seen in the OS of chick photoreceptors.[13] The iron-storage function for glial (Müller) cells was reported for chick retinas before and after hatching, although the authors did not exclude the IS of photoreceptors as candidates for iron stores.[13]

It is interesting to note that the studies on iron and iron-homeostasis protein distribution in humans, rodents, and avians showed the photoreceptor cells to be the most anti–Tf-immunoreactive structures. These cells are immunopositive for Tf-R, which suggests the Tf-R–dependent mechanism of iron delivery into the photoreceptors. Our data on the total heme and nonheme iron distribution in the adult rat retina show the presence of iron in both IS and OS of photoreceptors. An attempt to determine the total iron content in isolated rod outer segment disc membranes was made for the bovine retina.[36] According to the data obtained, the bovine retinal disc membranes contain iron as well as Cu and Zn. The latter has been shown to be bound with purified bovine rhodopsin.[37] As for iron, it would be extremely interesting to know in what valence and for what purpose it is present in the OS of photoreceptors. Is it bound to soluble ferritin, probably present here, or to the integral disc membrane proteins including rhodopsin? Because of the presence of a high amount of polyunsaturated fatty acids[38] in the disc membranes, it is likely that iron availability is tightly controlled. It is possible that the dysfunction of iron metabolism in the OS of photoreceptors could lead to the generation of free radical species that are able to destroy the photoreceptor membrane and induce dramatic events including photoreceptor cell death.[11] Iron indirect localization by EM studies indicates that most of it is present inside the disc of the native photoreceptors, but not on other membranes such as mitochondrial membranes, known to contain high levels of heme iron. This staining was also observed in the partially digested membranes inside phagosomes of the RPE layer, suggesting that there might be a recycling of iron. This will need to be confirmed. It raises further the necessity to identify to which protein(s) the iron is bound. It will also be interesting to analyze iron and iron homeostasis proteins in pathologic situations for a possible causal relationship. For example, in RCS rats with hereditary degeneration of the ret-

ina, phagocytosis is impaired and the retinal degeneration occurs at the same time (PN 20 to PN 55) as noted above.

Acknowledgments

The authors thank Mario Zakin for providing the rat Tf nucleotide sequence, Paolo Santambrogio for the gift of ferritin antibodies, Carole Beaumont for her advice, Laurent Jonet for his technical help in the immunohistologic experiments, and Hervé Coët for photographs.

References

1. Hentze MW, Kühn LC. Molecular control of vertebrate iron metabolism: mRNA-based regulatory circuits operated by iron, nitric oxide, and oxidative stress. *Proc Natl Acad Sci USA.* 1996; 93:8175–8182.
2. Zakin M. Regulation of transferrin expression. *FASEB J.* 1992;6: 3253–3258.
3. Pedersen O. An electron microscopic study of the permeability of intraocular blood vessels using lanthanum as a tracer in vivo. *Exp Eye Res.* 1979;29:61–69.
4. Schichi H. Microsomal electron transport system of bovine retinal pigment epithelium. *Exp Eye Res.* 1969;8:60–68.
5. Yau KW, Baylor DA. Cyclic GMP -activated conductance of retinal photoreceptor cells. *Annu Rev Neurosci.* 1989;12:2785–2802.
6. Becquet F, Courtois Y, Goureau O. Nitric oxide decreases in vitro phagocytosis of photoreceptor outer segments by bovine retinal pigmented epithelial cells. *J Cell Physiol.* 1994;159:256–262.
7. Nathan C, Xie QW. Nitric oxide synthases: roles, tolls and controls. *Cell.* 1994;78:915–918.
8. Fliesler SJ, Anderson RE. Chemistry and metabolism of lipids in the vertebrate retina. *Prog Lipid Res.* 1983;22:79–131.
9. Lakhanpal V, Schocket SS, Jiji R. Deferoxamine (Desferal®)-induced toxic retinal pigmentary degeneration and presumed optic neuropathy. *Ophthalmology.* 1984;91:443–451.
10. Rapp L, Wiegand RD, Anderson RE. Ferrous ion-mediated retinal degeneration: role of rod outer segment lipid peroxydation. In: Clayton RM, Haywood J, Reading HW, Wright A, eds. *Problem of Normal and Genetically Abnormal Retinas.* New York: Academic Press; 1982:109–119.
11. Wang ZJ, Lam KW, Lam TT, Tso MOM. Iron-induced apoptosis in the photoreceptor cells of rats. *Invest Ophthalmol Vis Sci.* 1998; 39:631–633.
12. Zeevalk GD, Hyndman AG. Transferrin in the chick retina: distribution and location during development. *Dev Brain Res.* 1987;37: 231–241.
13. Cho SS, Hyndman AG. The ontogeny of transferrin receptors in the embryonic chick retina: an immunohistochemical study. *Brain Res.* 1991;549:327–331.
14. Hyndman AG, Zeevalk GD. Transferrin and iron in cultured chick embryonic neurons: a comparison between human and chick transferrins. *J Cell Physiol.* 1988;134:238–244.
15. Hyndman AG. High affinity binding of transferrin in cultures of embryonic neurons from the chick retina. *Brain Res.* 1991;564: 127–131.
16. Hunt RC, Davis AA. Release of iron by human retinal pigment epithelial cells. *J Cell Physiol.* 1992;152:102–110.
17. Laicine EM, Haddad A. Transferrin, one of the major vitreous proteins is produced within the eye. *Exp Eye Res.* 1994;59:441–446.
18. Baudouin Ch, Brignole F, Fredj–Reygrobellet D, Negre Fl, Bayle J, Gastaud P. Tranferrin receptor expression by retinal pigment epithelial cells in proliferative vitreoretinopathy. *Invest Ophthalmol Vis Sci.* 1992;33:2822–2829.
19. Davis AA, Hunt RC. Transferrin is made and bound by photoreceptor cells. *J Cell Physiol.* 1993;156:280–285.
20. Sergeant C, Gouget B, Llabador Y, et al. Iron in hereditary retinal degeneration: PIXE microanalysis. Preliminary results. *Nucl Instr Methods B.* 1999;158:344–348.
21. Moretto P, Razafindrale L. Simulation of RBS spectra for quantitative mapping of inhomogenous biological tissue. *Nucl Instr Methods B.* 1995;104:171–175.
22. Maxwell JA, Campbell JL, Teesdale WJ. The Guelph PIXE software package. *Nucl Instr Methods B.* 1989;43:218–230.
23. Willingham MC, Rutherford AV. The use of osmium-thiocarbohydrazide-osmium (OTO) and ferrocyanide-reduced osmium methods to enhance membrane contrast and preservation in cultured cells. *J Histochem Cytochem.* 1984;32:455–460.
24. Cotter JR. Endocytosis of cationized ferritin by rat photoreceptors. *Neurosci Lett.* 1989;106:65–70.
25. Le Magueresse B, Pineau C, Guillou F, Jegou B. Influence of germ cells upon transferrin secretion by rat Sertoli cells in vitro. *J Endocrinol.* 1988;118:R13–R16.
26. Chirgwin JM, Preyzila AE, McDonald R, Rutter J. Isolation of biological active ribonucleic acid from sources enriched in ribonuclease. *Biochemistry.* 1978;18:5294–5299.
27. White DL, Mazurkiewicz JE, Barrnett RJ. A chemical mechanism for tissue staining by osmium tetroxide-ferrocyanide mixtures. *J Histochem Cytochem.* 1979;27:1084–1091.
28. Neiss WF. Electron staining of the cell surface coat by osmium-low ferrocyanide. *Histochemistry.* 1984;80:231–242.
29. Tripathi RC, Borisuth NSC, Tripathi BJ, Gotsis SS. Quantitative and qualitative analyses of transferrin in aqueous humor from patients with primary and secondary glaucomas. *Invest Ophthalmol Vis Sci.* 1992;33:2866–2873.
30. Laicine EM, Haddad A. Transferrin, one of the major vitreous protein is produced within the eye. *Exp Eye Res.* 1994;59:441–446.
31. Dickinson TK, Connor JR. Cellular distribution of iron, transferrin, and ferritin in the hypotransferrinemic (Hp) mouse brain. *J Comp Neurol.* 1995;355:67–80.
32. Moos T. Immunocytochemical localization of intraneuronal transferrin receptor immunoreactivity in the adult mouse central nervous system. *J Comp Neurol.* 1996;375:675–692.
33. Bruininc A, Cidler C, Birchler F. Neurotrophic effects of transferrin on embryonic chick brain and neural retina cell cultures. *Int J Dev Neurosci.* 1996;14:785–795.
34. Hyndman AG, Hockberger PE, Zeevalk GD, Connor JA. Transferrin can alter physiological properties of retinal neurons. *Brain Res.* 1991;561:318–323.
35. Friedman AH, Gartner S, Modi SS. Drusen of the optic disc: a retrospective study in cadaver eyes. *Br J Ophthalmol.* 1975;59: 413–421.
36. McCormick LD. Bound trace element content of bovine retinal disc membranes as determined by particle-induced X-ray emission. *Biophys J.* 1985;47:381–385.
37. Shaster TA, Nagy AK, Conly DC, Farber DB. Direct zinc binding to purified rhodopsin and disc membranes. *Biochem J.* 1992;282: 123–128.
38. Fliesler SJ, Anderson RE. Chemistry and metabolism of lipids in the vertebrate retina. *Prog Lipid Res.* 1983;22:79–131.